

Effect of Polymer Architecture and Ionic Aggregation on the Scattering Peak in Model Ionomers

Lisa M. Hall,¹ Mark J. Stevens,^{1,2} and Amalie L. Frischknecht^{1,2,*}

¹*Computational Materials Science and Engineering Department, Sandia National Laboratories, Albuquerque, New Mexico 87185, USA*

²*Center for Integrated Nanotechnologies, Sandia National Laboratories, Albuquerque, New Mexico 87185, USA*
(Received 21 December 2010; published 23 March 2011)

We perform molecular dynamics simulations of coarse-grained ionomer melts with two different architectures. Regularly spaced charged beads are placed either in the polymer backbone (ionenes) or pendant to it. The ionic aggregate structure is quantified as a function of the dielectric constant. The low wave vector ionomer scattering peak is present in all cases, but is significantly more intense for pendant ions, which form compact, discrete aggregates with liquidlike interaggregate order. This is in qualitative contrast to the ionenes, which form extended aggregates.

DOI: 10.1103/PhysRevLett.106.127801

PACS numbers: 61.41.+e, 36.20.Ey, 82.35.Cd

Ionomer melts, polymers with a small fraction of charged groups and no solvent, are of interest as novel battery electrolytes, among other applications. Without screening of Coulombic interactions by solvent, strong ion-ion interactions can yield aggregates of ions. These lead to interesting mechanical properties, but potentially hinder counterion transport. A characteristic feature of ionomers associated with the length scale of ionic aggregation is a low wave vector peak in the scattering. The underlying microstructure has been debated for decades, and several competing models [1–3] are currently used to fit the peak. There has been relatively little guidance from other experiments (microscopy provides important information, but a typical image shows a 2D projection of many overlapping aggregates) [4,5] or from simulations to confirm or refute such models and interpret the specific structural meaning of the ionomer peak.

The Yarusso-Cooper and related models are popular methods of fitting the ionomer peak [1,2,5–7], and propose that spherical regions of increased ion density (aggregates) pack like hard spheres of a larger size (the radius of closest approach). Recent scattering measurements of ionomers with a precise spacing of anions along the polymer chain show their ionomer peak is much stronger than that of randomly spaced analogs, indicating a relatively high degree of interaggregate order [4,5]. Analysis of micrographs reinforces the model of spherical aggregates for this system [5]. These materials present an obvious starting point for modeling. We present molecular dynamics (MD) simulations of two coarse-grained models of ionomers with precisely spaced charges, having periodically spaced charged beads either within (ionenes) or pendant to the polymer backbone, which lead to qualitatively different morphologies. The results provide a detailed picture of the order within and among ionic aggregates and the resulting scattering peak.

Most previous theoretical and simulation studies of ionomers have focused on hydrated membranes of interest in

fuel cell applications [8]. Water changes the aggregation behavior and is avoided in batteries. One group has simulated a dry ionomer, still considering the specific chemistry typical of fuel cell membranes and not including free counterions [9]. Modeling dry ionomers with explicit counterions, which influence aggregation and are especially relevant for battery applications, has rarely been done. Coarse-grained MD simulations of polymers with ions on the ends of the chain (telechelics) [10] and periodically spaced in the chain backbone (ionenes) [11], including counterions, have been performed. The latter system is similar to our ionene model, but those simulations were small and focused on glass transition behavior.

We performed simulations on large systems which for the first time clearly resolve the ionomer peak and average aggregate behavior. When the charged groups are pendant to the polymer backbone rather than part of the backbone, the ionomer peak is sharper. We demonstrate that the pendant peak length scale corresponds to liquidlike ordering between discrete aggregates.

We employ a bead-spring polymer model [12]. A unit of 9 backbone beads is repeated 4 times per chain. The middle bead of the repeat unit is either charged (the ionene architecture) or is bonded to a charged pendant bead. Other polymer beads are uncharged, and an equal number of oppositely charged counterions are added. We use typical Kremer-Grest parameters [12,13]; all beads interact through a repulsive Lennard-Jones (LJ) potential with $\epsilon_{LJ} = 1.0$ shifted to zero at its minimum, and adjacent beads are connected by the finitely extensible nonlinear elastic potential with $R_0 = 1.5$ and $k = 30$ (LJ units). The LJ diameter of all polymer beads is 1.0σ while the counterion diameter is 0.5σ and the cross interaction is additively mixed. All beads and counterions have unit mass. A bead of this model maps approximately to three CH_2 units in a polyethylene backbone [13], which also corresponds to the size of a COO^- group [14] and yields $\sigma \sim 0.4$ nm.

Our counterion diameter maps approximately to the ionic diameter of $\text{Na}^+ \sim 0.2$ nm.

Long-range electrostatics were fully accounted for with the particle-particle particle-mesh method in the LAMMPS MD code [15]. A Langevin thermostat is used with a dimensionless damping constant of 1.0 and constant reduced temperature $T^* = kT/\epsilon_{\text{LJ}} = 1$. The dielectric constant of the medium ϵ_r is inversely proportional to the Bjerrum length, $l_B = q^2/(4\pi\epsilon_0\epsilon_r kT)$, the distance at which the Coulomb interaction equals kT , where ϵ_0 is the vacuum permittivity and q is charge. The dimensionless quantity σ/l_B was varied from 0.014 to 0.070 in increments of 0.014. This corresponds to ϵ_r of 2 to 10, which approximately mimics the range of typical ionomer backbone chemistries from polyethylene to poly(ethylene oxide). The system packing fraction $\eta_t = (\rho_{\text{CI}}(0.5\sigma)^3 + \rho_{\text{B}}\sigma^3)\pi/6$ was set to $0.7\pi/6 = 0.366$, in the range typical of polymer melts, where ρ represents number density and the subscripts CI and B stand for counterions and polymer beads, respectively. The cubic simulation box contained 800 polymers and 3200 counterions, giving a side length of 34.7σ for ionenes or 35.9σ for pendants. Polymers and counterions were placed in the box randomly and equilibrated for 10^7 time steps of 0.005τ , where τ is the LJ time unit. Data were obtained for an additional 4×10^7 time steps.

Periodically during the simulation time, the mean squared displacement (MSD) of polymer centers of mass and of counterions was calculated after subtracting the small total system center-of-mass displacement. These MSDs were each linear in time by the end of the simulation for all but the lowest $\epsilon_r = 2$. The related systems considered in Refs. [10,11] each showed a glass transition at σ/l_B between that of our $\epsilon_r = 2$ and 4 systems. We also find that the $\epsilon_r = 2$ system is glassy; the polymer center of mass MSD is less than 1.5σ and the counterion MSD is less than 3σ by the end of the simulation for both the pendant and ionene architectures. In the remainder of this letter we discuss well equilibrated, diffusive $\epsilon_r \geq 4$ systems. At $\epsilon_r = 4$, the counterion MSD of the pendant systems is $\sim 200\sigma$ and that of ionenes is $\sim 1500\sigma$ by the end of the simulation, while the analogous polymer center of mass MSDs are 30σ and 250σ . Analysis of counterion and aggregate dynamics will be reported in a future publication.

To examine the structure we calculated partial pair correlation functions $g_{ij}(r)$ from 400 configurations using the visualization software VMD, which was also used to create images [16]. Partial structure factors $S_{ii}(k) = 1 + \rho_i h_{ii}(k)$ were calculated from a Fourier transform of $h_{ij}(r) = g_{ij}(r) - 1$. Cluster (aggregate) analysis was performed on 101 configurations in the first quarter of the simulation time by grouping any oppositely charged ions within a distance of 0.9σ of each other into the same aggregate, and then by tallying the number of ions in and calculating the spatial extent of each resulting aggregate.

TABLE I. Aggregate and ionomer peak data: the mean n_{agg} and standard deviation σ_{agg} of ionic aggregate size (number of counterions and charged beads) and the height $S_{\text{CI-CI}}(k^*)$ and wave vector k^* of the ionomer peak in the counterion structure factor.

| Architecture | ϵ_r | n_{agg} | σ_{agg} | $S_{\text{CI-CI}}(k^*)$ | $k^*(\sigma^{-1})$ |
|--------------|--------------|-------------------|-----------------------|-------------------------|--------------------|
| Ionenes | 4 | 33.2 ^a | 42.0 ^a | 5.0 | 1.4 |
| Ionenes | 6 | 13.9 | 18.3 | 2.5 | 1.4 |
| Ionenes | 8 | 5.3 | 5.0 | 1.7 | 1.5 |
| Ionenes | 10 | 3.3 | 2.7 | 1.4 | 1.5 |
| Pendants | 4 | 30.8 | 10.9 | 15.4 | 1.2 |
| Pendants | 6 | 20.3 | 20.3 | 5.7 | 1.2 |
| Pendants | 8 | 7.2 | 7.4 | 2.9 | 1.2 |
| Pendants | 10 | 4.1 | 3.8 | 2.0 | 1.4 |

^aSome aggregated ionic structures of ionenes at $\epsilon_r = 4$ are percolated. For this system 76% of ions are in the one or two structures which span the box and are not included as “aggregates.”

The cluster analysis revealed ionic aggregates in all systems; their sizes are reported in Table I. At $\epsilon_r = 4$, the pendant system forms discrete aggregates with a narrow size distribution, as quantified by the small standard deviation in the mean aggregate size (note $\sigma_{\text{agg}} < n_{\text{agg}}$). The ionenes form a fundamentally different structure at $\epsilon_r = 4$, with a large percolated ionic aggregate that spans the system. Ionene aggregates other than the percolated structure are of a wide variety of sizes, with $\sigma_{\text{agg}} > n_{\text{agg}}$. Increasing ϵ_r destroys the ionenes’ percolated structure and decreases aggregate size. At high ϵ_r , the ionene and pendant systems show relatively similar behavior. We therefore focus on the well ordered case of $\epsilon_r = 4$ where polymer architecture has the greatest effects.

Snapshots of the ionene and pendant systems at $\epsilon_r = 4$ also show their different morphologies (Fig. 1). The pendant aggregates are compact, while ionene aggregates are more extended or stringlike. In our fully neutralized ionomer model, aggregates are dense ion-only structures, rather than regions of relatively higher ion density that also include polymer backbone as proposed experimentally to reconcile the size of aggregates in the Yarusso-Cooper model fit with calculated ionic volume fractions [2,6,7]. Even at $\epsilon_r = 10$ (not shown) where single ions are common, the small stringlike or globular aggregates that do exist exclude uncharged polymer segments. The Eisenberg-Hird-Moore ionomer model proposes dense multiplets but does not include the liquidlike interaggregate ordering we find in the pendant system [3]. We also do not observe “core-shell” aggregates [1]: we find nearly pure polymeric and ionic regions, but not surrounding regions of intermediate ion density.

The counterion-counterion scattering structure factors of the ionene and pendant systems at $\epsilon_r = 4$ are shown in Fig. 2; the charged bead-charged bead structure factors

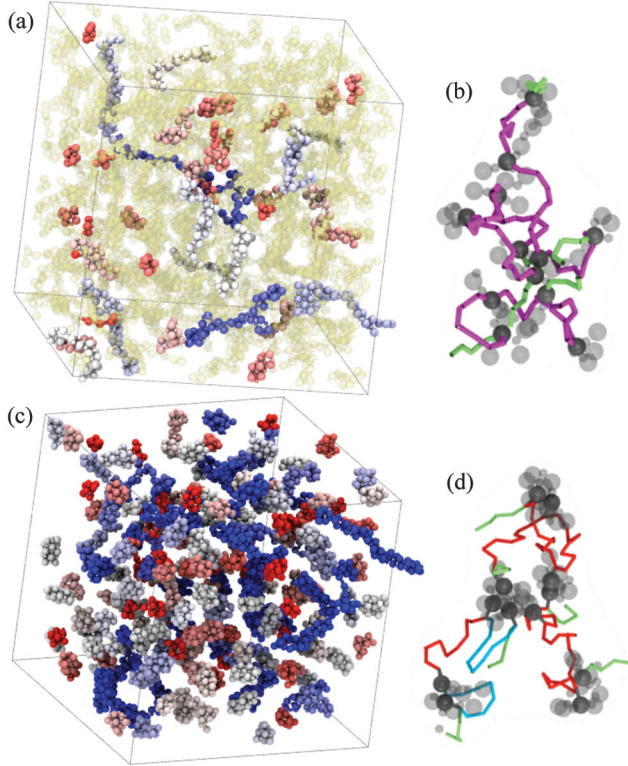


FIG. 1 (color). Snapshots of ionenes [(a) and (b)] and pendants [(c) and (d)] at $\epsilon_r = 4$. Snapshots (a) and (c) show only the charged beads and counterions in one simulation box. Results of a cluster analysis were used to color the images; the percolated structure of the ionene system is transparent yellow, while other aggregates are colored from red to white in order of increasing aggregate size. Aggregates are each drawn contiguously with the aggregate center-of-mass in the given periodic box. Images (b) and (d) are of three selected nearby polymers showing loops and bridges between aggregates. Tubes represent bonds, charged beads are gray spheres, and any other charged beads and counterions within 1.5σ of these polymers are transparent gray. Polymer end segments are green, segments between charged beads which bridge between aggregates are red, those looping back closely within an aggregate are blue, and those looping back within the percolated structure are magenta.

are nearly identical (not shown). The pendant system's peak is extremely sharp. The peak is at the same wave vector as its aggregate center-of-mass to center-of-mass ordering peak (calculated from cluster analysis results and shown by the dash-dotted line), similar to the assumption of Yarusso-Cooper type models. Using the map to nm, the peak position is $\sim 3.0 \text{ nm}^{-1}$, in the range of experimental results on related materials [5,6]. The ionene system's peak is significantly smaller and instead corresponds to the long-range order within its percolated ionic structure. Increasing ϵ_r decreases aggregation and the height of the ionomer peak (Table I).

The charged bead (CB)—counterion (CI) and CI-CI pair correlation functions are shown in Fig. 3 for ionenes and pendants at low and high ϵ_r . $g_{\text{CB-CB}}(r)$ is very similar to

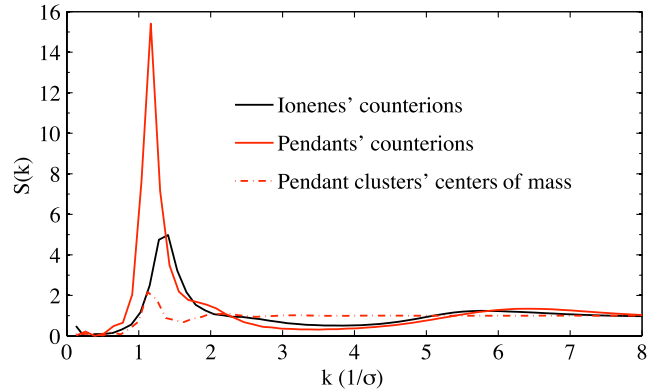


FIG. 2 (color online). Partial structure factors for pendant and ionene architectures at $\epsilon_r = 4$.

$g_{\text{CI-CI}}(r)$ and is not included. The first CB-CI peak is at $\sim 0.75\sigma$, the CB-CI contact distance, while the first two CI-CI peaks are at $\sqrt{2}$ and 2 times this distance (the first of which becomes a shoulder at $\epsilon_r = 10$). These latter two are the distances between like charges in a planar quadrupole and in linear triplets of ions, respectively. At high ϵ_r , Coulomb interactions and the associated local order are weak, and the second peak in $g_{\text{CI-CI}}(r)$ becomes stronger than the first, signaling that linear $- + - + -$ (or longer) arrangements are relatively more prevalent than squarelike configurations in compact structures. The pendants and ionenes have slightly different locations of their other short range peaks, as the pendants form more compact structures while the ionene aggregates are more stringlike. These differences are diminished at high ϵ_r .

A long-range peak occurs at $\epsilon_r = 4$ that is significantly more intense and longer range for pendants than for

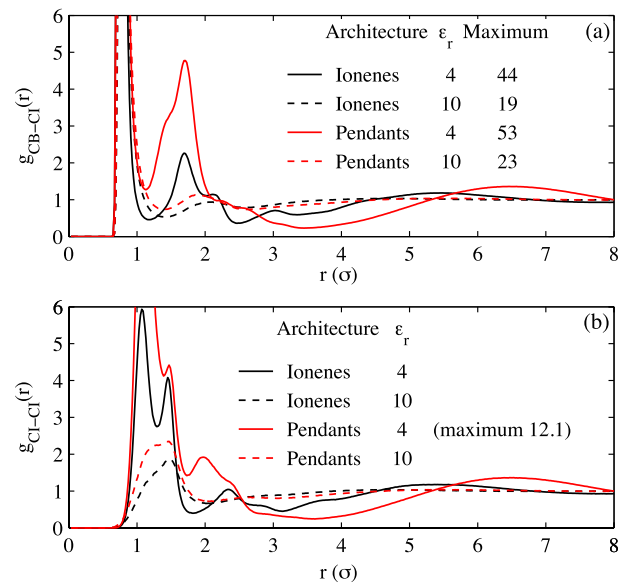


FIG. 3 (color online). (a) Charged bead-counterion and (b) counterion-counterion pair correlation functions for the noted architecture and ϵ_r .

ionenes and corresponds to the ionomer peak in $S(k)$. This feature is nearly identical in $g_{\text{CB-Cl}}(r)$, $g_{\text{Cl-Cl}}(r)$, and $g_{\text{CB-CB}}(r)$ (not shown), suggesting an overall length scale of ordering of both counterions and charged beads. In the pendant case, this corresponds to interaggregate order, while in the ionene case this corresponds to mesoscale ordering within the large percolated structure. Both local and long-range order is stronger in the pendant case. Being bonded to 1 instead of 2 uncharged beads, the pendant can associate with a greater number of surrounding nearest neighbor ions. The pendant charged bead can also potentially insert itself into an aggregate with less loss of polymer entropy since its backbone does not enter into the structure as it must in the ionene case. Thus, both enthalpic and entropic considerations apparently favor more compact aggregates in the pendant ionomers versus the ionenes, leading to their qualitatively different ionic aggregate morphologies.

The polymer backbone is intimately involved in the spacing between aggregates, as exhibited by the conformations of 3 selected ionene and pendant polymers shown in Figs. 1(b) and 1(d), respectively. Polymer backbone segments connecting adjacent charged beads are identified as either bridges between different aggregates or loops back into the same aggregate (or back into the same percolated structure) during our cluster analysis, and loops are categorized as “close loops” if their charged beads are within a distance of 1.8σ . For pendants at $\epsilon_r = 4$, 74% of backbone segments are bridges, helping to set the interaggregate length scale. With fewer discrete aggregates in the ionenes, only 30% of segments are bridges. Two nearby close loops can set the interaggregate distance similar to a backbone bridge as shown in Fig. 1(d). Close loops make up 20% of backbone segments for pendants at $\epsilon_r = 4$, while only 6% of segments loop further away but within an aggregate. This reflects the increased polymer ordering in this system versus ionenes, which have only 15% close loops.

We considered several related systems to ensure the accuracy of our results. A very large box containing 6400 pendant polymers ($\sim 2.8 \times 10^5$ total beads and counterions) was simulated at $\epsilon_r = 4$, and finite box size effects were seen to be very small. For this system of 6400 polymers and all other systems with 800 polymers per box, all ion-ion $g_{ij}(r)$ oscillate within 1% of unity by half of the box length. Density was varied up to $0.85\pi/6$ at $\epsilon_r = 4$ in initial calculations using 100 polymers per box. The resulting $g_{ij}(r)$ and $S_{ij}(k)$ were qualitatively very similar to those at $0.7\pi/6$, but increasing density slowed down equilibration, and by $\eta_r = 0.85\pi/6$, full equilibration was not reached during the time scale of the simulation. The $\epsilon_r = 4$ systems started from different random initial configurations did not show noticeable differences in $g_{ij}(r)$ on the scale of the figures presented here.

We have shown that simple molecular models of precisely spaced, fully neutralized ionomers yield a strong

ionomer peak at low dielectric constant. Qualitatively different ionic aggregate structures can give rise to similar ionomer peaks in the scattering. The pendant architecture shows a very sharp peak and significant liquidlike order between its well-defined aggregates. In contrast, the ionene system’s peak corresponds to mesoscale order within a percolated ionic structure. Simulations thus give a more detailed molecular picture of ionic structures in ionomers than can be obtained experimentally.

We thank Karen Winey and Michelle Seitz for helpful discussions and Karen Winey for comments on the manuscript. This work is supported by the Sandia LDRD program. This work was performed, in part, at the Center for Integrated Nanotechnologies, a U.S. Department of Energy, Office of Basic Energy Sciences user facility. Sandia National Laboratories is a multiprogram laboratory operated by Sandia Corporation, a Lockheed Martin Company, for the U.S. Department of Energy under Contract No. DE-AC04-94AL85000.

*alfrisc@sandia.gov

- [1] A. Eisenberg and J.-S. Kim, *Introduction to Ionomers* (Wiley, New York, 1998).
- [2] D.J. Yarusso and S.L. Cooper, *Macromolecules* **16**, 1871 (1983).
- [3] A. Eisenberg, B. Hird, and R. B. Moore, *Macromolecules* **23**, 4098 (1990).
- [4] T.W. Baughman, C.D. Chan, K.I. Winey, and K.B. Wagener, *Macromolecules* **40**, 6564 (2007).
- [5] M.E. Seitz, C.D. Chan, K.L. Opper, T.W. Baughman, K.B. Wagener, and K.I. Winey, *J. Am. Chem. Soc.* **132**, 8165 (2010).
- [6] N.M. Benetatos, C.D. Chan, and K.I. Winey, *Macromolecules* **40**, 1081 (2007).
- [7] N.C. Zhou, C.D. Chan, and K.I. Winey, *Macromolecules* **41**, 6134 (2008).
- [8] D. Galperin, P.G. Khalatur, and A.R. Khokhlov, *Device and Materials Modeling in PEM Fuel Cells*, edited by S.J. Paddison and K.S. Promislow, Topics in Applied Physics Vol. 113 (Springer, New York, 2009), p. 453.
- [9] E. Allahyarov and P.L. Taylor, *J. Chem. Phys.* **127**, 154901 (2007).
- [10] M. Goswami, S.K. Kumar, A. Bhattacharya, and J.F. Douglas, *Macromolecules* **40**, 4113 (2007).
- [11] C. Wong and J.H.R. Clarke, *J. Chem. Phys.* **116**, 6795 (2002).
- [12] *Monte Carlo and Molecular Dynamics Simulations in Polymer Science*, edited by K. Binder (Oxford, New York, 1995).
- [13] K. Kremer and G.S. Grest, *J. Chem. Phys.* **92**, 5057 (1990).
- [14] G. Kamath, F. Cao, and J.J. Poto, *J. Phys. Chem. B* **108**, 14130 (2004).
- [15] S. Plimpton, *J. Comput. Phys.* **117**, 1 (1995).
- [16] W. Humphrey, A. Dalke, and K. Schulten, *J. Mol. Graphics* **14**, 33 (1996).